CASTANEA 88(2): 161–175 June

A Novel Anatomical Approach to Complement Morphological and Ecological Methods for the Identification of Some Important Coastal Graminoids

Anubhav Thapaliya, Hee So, Sarah Fones, Sarah McCrimmon, Mia Wyche, Joseph Battistelli, and Sierra Beecher*
Virginia Commonwealth University, Eugene P. and Lois E. Trani Center for Life Sciences, Suite 126, 1000 W. Cary St., Richmond, VA 23284

ABSTRACT

We present anatomical imaging techniques and measurements that are useful additions to the existing morphological toolbox for the identification of seven coastal grasses and one rush. Our method is simple and inexpensive and requires the removal of only one leaf, which prevents removal of plants from their habitats. This method can also be used in seasons when reproductive structures (important for current morphological ID efforts) are not present. We find significant quantitative differences in leaf width, adaxial to abaxial ratios (ADAB ratio, which we introduce as a new parameter), vascular bundle cross-sectional areas, and interveinal distances, as well as providing images for qualitative analysis of these plants' anatomies; including differences in bundle sheath structures, fiber distributions, epidermal and cuticular properties, and chloroplast positioning.

Key words: C4 photosynthesis, dune building, leaf anatomy, salt marsh grass, vascular bundle

List of abbreviations for measurements
ADAB Ratio: The length of the adaxial side of the leaf in transverse section divided by the length of the abaxial side.
AVB: Area of vascular bundles. The cross-sectional area of vascular bundles.
IVD: Interveinal distance. The distance between vascular bundles in transverse section.
Wmin: The minimum width of the leaf. An average of technical and biological replicates.
Wmax: The maximum width of the leaf. An average of technical and biological replicates.
Plant list including USDA abbreviations
AMBR—*Ammophila breviligulata* Fernald. **DISP**—*Distichilis spicata* (L.) Greene. **JUGE**—*Juncus gerardii* Loisel. **PAAM**—*Panicum amarum* Elliott. **PHAU**—*Phragmites australis* (Cav.) Steud. **SPAL****—*Spartina alterniflora* Loisel. **SPPA**—*Spartina patens* (Aiton) Muhl. **UNPA**—*Uniola paniculata* L.

**The tall and short varieties of this species were analyzed separately and compared. Plants are referred to by their USDA abbreviations in graphs depicting measurements and figures.

INTRODUCTION

Coastal wetlands are a crucial part of the florasphere, providing numerous ecosystem services including flood protection, storm surge buffering, sea level rise mitigation, fish nurseries, migrating bird habitat, dune building, and bank stabilization (Feagin et al. 2015; Hacker et al. 2019). Many plant members of these communities are of scientific interest beyond their local ecological services, because of their myriad adaptations for success in extreme environments, especially salinity (and therefore

*email address: sdbeecher@vcu.edu
Received 28 October 2022; Accepted 1 June 2023

aridity) tolerance (Rozema et al. 2014), nutrient limitations, inundation, and the ability to deal with wind. Some researchers have examined the utility of genes and anatomies in these plants for crop improvement in degraded and saline soils (Chung 2006; Chen et al. 2015; Srinivas et al. 2018), and for their potential in biofuel production (Christian et al. 2002). Finally, some of these plants are used as animal fodder and construction materials (Mehaffey et al. 2005). Therefore, the restoration and conservation of coastal wetlands is important, and has the potential to yield economic and ecological benefits. The ecosystem services provided by these plants are related to their anatomies, and many have diagnostic, taxonomically useful microscopic characteristics that are described in part here.

Many of the members of coastal wetland plant communities are grasses. These monocots can be challenging to identify, because the reproductive parts, which are important phenotypic markers, are not always present, and using other morphological indices requires presence of multiple parts of the plant, including the flowers (Tiner 1987). Being able to identify and distinguish these plants efficiently is necessary for effective conservation and restoration efforts. Although graminoids have many phenotypic similarities, they inhabit very specialized niches, and the Ecological Species Concept (Crain et al. 2004) is highly applicable (Figure 1). When doing plant community surveys, accurate identification and the ability to screen for invasives is needed, and when doing restoration work, it is important to consider their specialized niches to maximize benefits. Here we propose a simple, low-cost method to aid in coastal graminoid identification using standard light microscopy with fresh hand-sectioning that does not require embedding, staining, or specialized equipment. We hope that this information will be useful for those involved in coastal restoration efforts, including seed bank workers. Our methods could also be employed to efficiently screen for some anatomical changes caused by ecological fluxes and genetic variation in these and other plants. Much has been written about the ecological significance of these plants, but a brief summary of each is below, as well as some previously discovered anatomical features.

Distichlis spicata L. Greene

Distichlis spicata (L.) Greene (salt grass) is a recretohalophytic dioeceous plant that is native and widespread in the United States and a common inhabitant of the mid-high salt grass marsh and hind dune communities (Litalien et al. 2020). Its recretohalophytic nature has been explored as a means for phytoremediation in soils that are degraded by salinity intrusion (Morris et al. 2019). In salt grass marshes, it provides valuable ecosystem services as a source of food for larval insects, pollution and erosion prevention via extensive root systems, and provides habitat for birds and small mammals (Lonard and Judd 2011). Anatomical identifying traits include Kranz anatomy (bundle sheath with chloroplasts), fibers encircling the vascular bundles and distributed throughout the phloem, salt extrusion structures, water collection cells lacking chloroplasts, ridges, and papillae (Figure 2). Semenova et al. (2010) noted all these, and Hansen et al. (1976) also reported stomata receded under papillae on the adaxial leaf surface, using scanning electron microscopy (SEM). Our method for this paper was not sufficient to identify stomata with certainty, but other structures were found and identified.

Ammophila breviligulata Fernald

Ammophila breviligulata Fernald (American beachgrass) is an important pioneer species in dune evolution. Its dense shoots and rapid spread facilitate the construction of foredunes. As such, it is a major part of the plant community that is responsible for foredune formation on the mid-Atlantic U.S. coast (Hacker et al. 2019). Its root systems are very important as well in provision of valuable ecosystem services such as accretion and coastal protection (Barbier et al. 2011), and for its function as a pioneer species. Charbonneau and Balsamo (2015) found similar structures in leaf anatomy as we did using SEM. Although their images showed slightly larger Wmax values, the ADAB ratio we measured in their image and the qualitative structure were quite comparable to our compound light micrographs.

Spartina alterniflora Loisel

Spartina alterniflora Loisel (smooth cordgrass) is an important member of salt marsh communities.

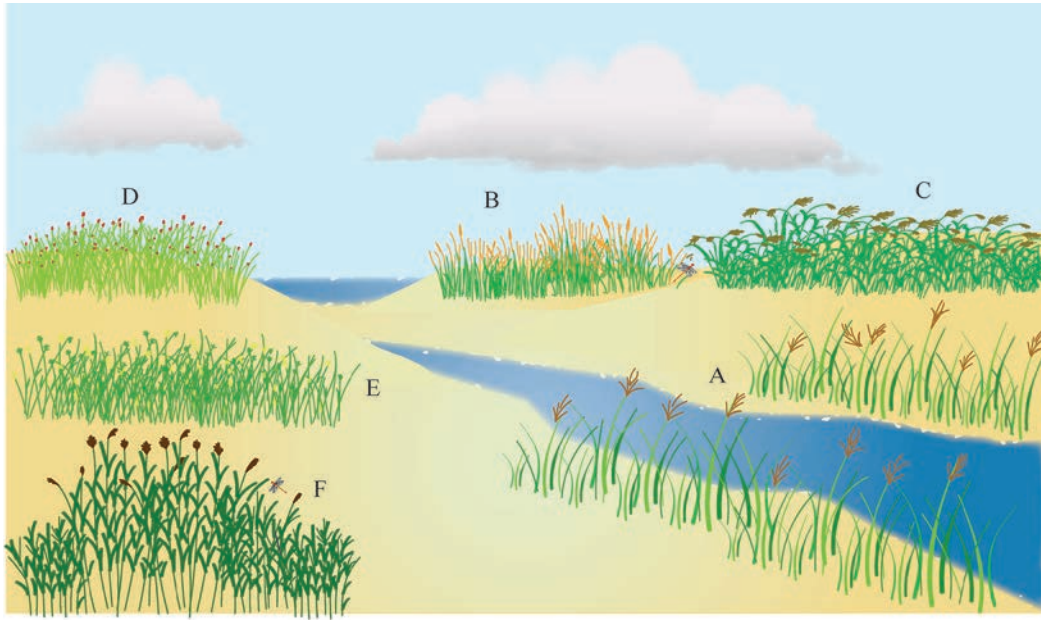

Figure 1. Digital artistic representation of habitats of grasses in this study. Marsh and beach grasses are found in zones, making the ecological species concept (ESC) useful for identification (Crain et al. 2004). **A.** *Spartina alterniflora* (C4): inhabits salt marsh creek edges, high tolerance for salinity and inundation. Provides habitat for migrating terns, willets, and several mollusks and crustaceans. **B.** *Ammophila breviligulata* (C3): inhabits coastal beaches and dunes. Pioneer dune building species can tolerate high wind, low water availability, and forms mutualistic relationship with mycorrhizae for nitrogen uptake. **C.** *Panicum amarum* (C4): dune building functions in aft dunes, high rate of growth, of interest for crop development. **D.** *Juncus gerardii* (C3): salt tolerant rush. Grows in salt marsh meadows with *Spartina patens* (C4) and **E.** *Distichlis spicata* (C4), higher in the marsh than *S. alterniflora*. **F.** *Phragmites australis* (C3): high growth rate, limited by salinity and shade, can be invasive in disturbed areas.

This plant has an extreme tolerance for salinity thanks to its salt excretion structures, specialized molecular ion selectivity (Baisakh et al. 2012), C4 photosynthetic apparatus, and positioning of stomata (Maricle et al. 2009). These anatomical and physiological properties not only contribute to its important ecosystem services, but also place it at high value as a candidate for ecological engineering (Chung 2006) and crop improvement efforts, especially in salinized and degraded soils (Ye et al. 2020). Previous work by Maricle et al. (2009) revealed similar structures and measurements as our results, and provided a means to test the rigor of our measurements on both *S. alterniflora* and *S. patens*. We found significant differences in IVD and Wmax (p<0.001) between the short and tall varieties of this species.

Spartina patens (Aiton) Muhl.

Spartina patens (Aiton) Muhl. (salt meadow cordgrass) is a dominant member of the higher marsh in many coastal grass communities. It often forms mats in the salt marsh meadow that are swirled from wind activity, which is an identifying characteristic of its habit. Its leaf anatomy is striking, with large lobed structures made of colorless parenchyma cells on the adaxial side, superior to the vascular bundles. The adaxial epidermis contains "zipper like" cuticular extensions and many simple trichomes (See Figure 3). It is a C4 plant with a moderate salinity tolerance. Kranz anatomy is apparent in large, chloroplast-containing bundle sheath cells, and unique oblong cells in transverse section can be seen inferior to the phloem. Below this is a fiber bundle. A uniform cuticle is apparent on the abaxial epidermis. Maricle et al. (2009) noted similar structures, and their leaf width measurements were consistent with ours.

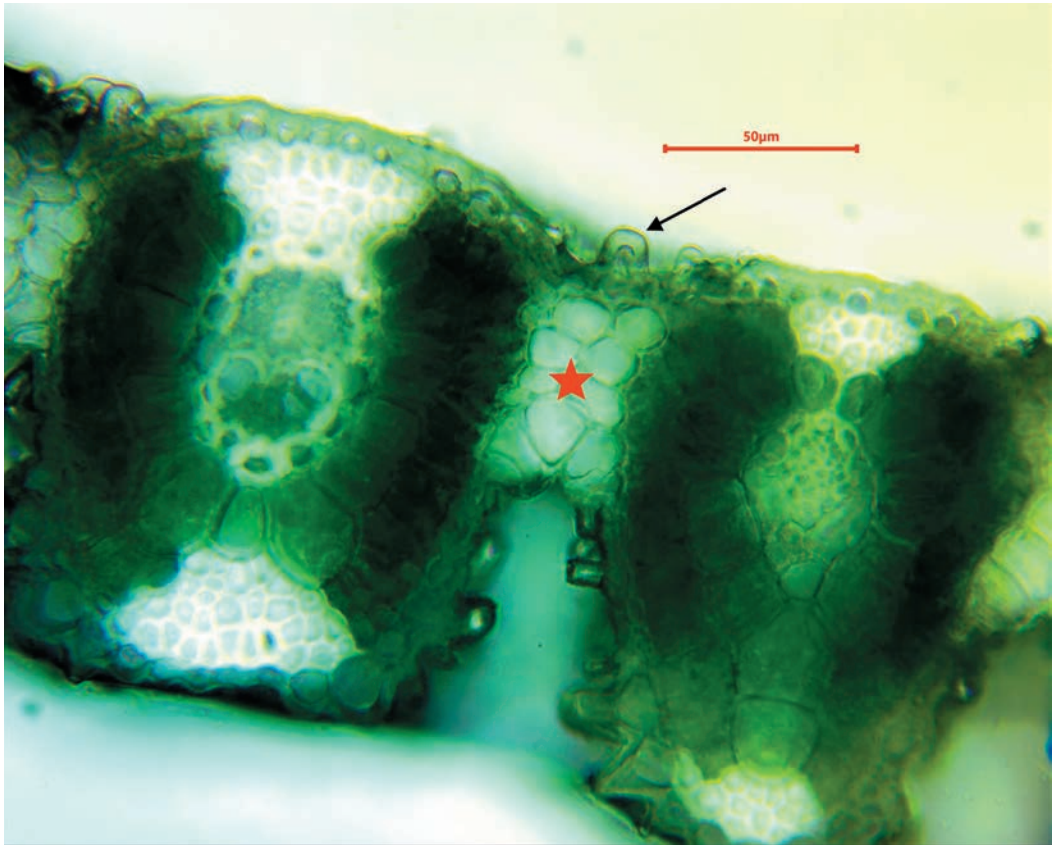

Figure 2. Salt glands on abaxial side of the leaf (black arrow) and water collection cells (red star) in *Distichlis spicata* described by Semenova et al. (2010). Phloem is sclerosed, as described by Metcalfe (1960).

***Phragmites australis* (Cav.) Steud.**

Phragmites australis (Cav.) Steud. (common reed) has historically been a native member of wetland plant communities, but its abundance in the last 150 years has dramatically increased to a level of concern (Saltonstall 2002). It is thought that this expansion is related to anthropogenic changes in the environment and/or a cryptic invasion by a new, more aggressive haplotype (Saltonstall 2002). Because of the negative effects on biodiversity and nesting habitat area that this expansion is incurring, it is considered an invasive species (USFWS). However, it may be performing some ecosystem services such as facilitating the breakdown of "forever chemicals" in sediments by the rhizosphere community it supports (Toyama et al. 2011) and reducing eutrophication rates by acting as a sink for nitrogenous wastes (Eid et al. 2020). Guda et al. (2019) also noted several similar anatomical features to those that we report, although they referred to what we call bulliform cells as "motor cells". Their images also show a bundle sheath devoid of chloroplasts, variation in vascular bundle cross-sectional area, and leaf thickness measurements in the range of those that we obtained.

***Panicum amarum* Elliott**

Panicum amarum Elliott (bitter panicum) is a coastal grass native to Eastern North America. It has important roles in sand capture for foredune formation and is one of four most abundant grasses providing this important ecosystem service (Hacker et al. 2019). Similar sclerenchyma and

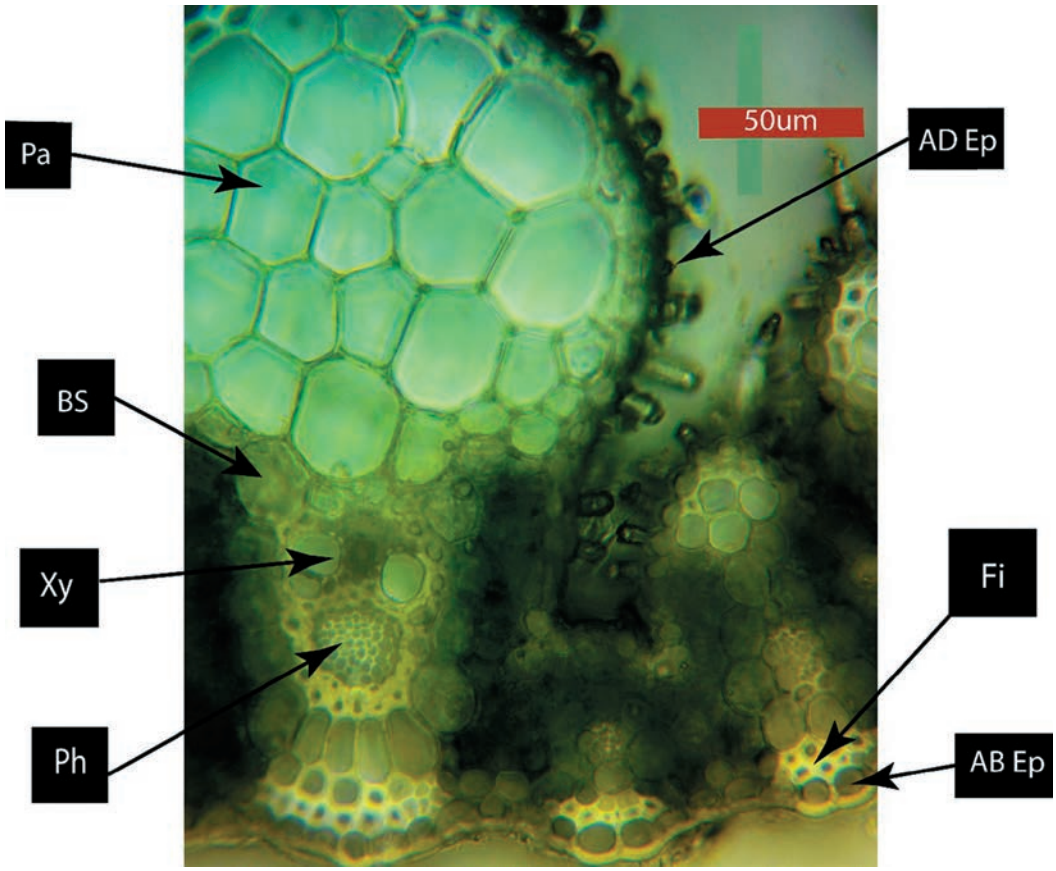

Figure 3. 40X image of S. patens. Pa=colorless parenchyma, BS Bundle sheath, Xy xylem, Ph phloem, AD Ep adaxial epidermis, Fi Fibers, AB Ep abaxial epidermis.

bulliform cell arrangements as we report were also found in previous anatomical research of members of this genus (Ohsugi and Murata 1986).

***Juncus gerardii* Loisel**

Juncus gerardii Loisel (salt meadow rush) is a salt tolerant rush that we found associated with *Spartina patens* and *Distichlis spicata*. It occupies higher marsh sites, and faces risks from flooding and sea level rise (Watson et al. 2014). Previous workers found qualitatively similar features, such as well-developed columnar bulliform cells, vascular bundle extensions, aerenchyma between vascular bundles, and sclerenchyma fibers positioned adaxially to vascular bundles (Grigiore and Toma 2011; Futorna and Olshanskyi 2013).

***Unioloa paniculata* L.**

Uniola paniculata L. (sea oats) is an important coastal grass of the southeastern coast of the Americas that provides many ecosystem services, including dune building. It can tolerate low moisture, low nutrients, high winds, high heat and salinity, and is a crucial germplasm resource for seed bank restoration work (Aracama et al. 2008). Aracama et al. (2008) also provided transmission electron micrographs of transverse sections of this plant's leaves at a similar scale as ours. We also observed high ADAB ratios, large Wmax values, and Kranz anatomy with chloroplast stacking in the bundle sheath cells.

MATERIALS AND METHODS

Sample collection

Leaf blades of *Spartina alterniflora, Spartina patens, Distichlis spicata, Juncus gerardii*, and *Phragmites australis* were collected from Cheesequake State Park in New Jersey. Leaf blades of *Ammophila breviligulata, Panicum amarum, Phragmites australis*, and *Spartina alterniflora* were collected at Old Bridge Waterfront Park in New Jersey. *Uniola paniculata* and *Panicum amarum* were collected at Virginia Beach barrier islands. Leaf blades were placed in water at the cut site and transported to the corresponding author's nearby "home office" for immediate microscopy.

Microscopy

Light microscopy of leaf transverse sections was performed using an Omax compound microscope, and imaging was accomplished with an OMAX 14MP trinocular digital camera (A3514OU) and ToupView software (ToupTek Photonics, Hangzhou, Zhejiang, P. R. China). Fresh hand sections were prepared with double-edged razors either freehand or using a Styrofoam block as described by Soukup and Tylová (2014) in section 1.3. These were imaged at 100 and 400X. No dyes or special spectral methods were employed.

Measurement

ImageJ (U.S. National Institutes of Health, Bethesda, Maryland) was used to measure leaf width, interveinal distance, area of vascular bundles, and the ratio between adaxial and abaxial lengths using methods similar to those employed by Savage et al. (2017) and checked by comparing measurements from previous imaging, which yielded similar values (Maricle et al. 2009). We formulated the ADAB ratio by using the freehand tool in ImageJ to estimate the length of the adaxial side of the leaf, and the abaxial side as: adaxial length/abaxial length as somewhat of a sinuosity index and an expression of dimorphic nature of the leaf anatomy (Figure 4). We measured widths at the widest parts of the leaf (Wmax) and the narrowest (Wmin) (Figure 5). This dimorphism enables the leaf to roll via an interlocking mechanism. This functionality also involves adaptations to the cuticle that reduces the surface area to volume ratio of the leaf and seals the stomata. These anatomical features minimize water loss allowing growth in extreme environments, providing high-value ecosystem services in doing so. Other plants we investigated employed a bulliform cell-based mechanism for rolling. These had lower ADAB ratios and require more water flux to function. We also report mean vascular bundle area (VBA) (Figure 6), and distance between bundles as interveinal distance (IVD) (Figure 5).

Art

Adobe Illustrator (Adobe.Inc) was used to create true-scale diagrams with the layering tool and customized palettes.

Statistical Analysis

Statistical analyses were performed with Microsoft Excel (Microsoft Inc. Redmond, Washington) and JMP (JMP®, Version 16. SAS Institute Inc., Cary, North Carolina), and graphs were created with SigmaPlot (SigmaPlot Version 12.3 (2013) Systat Software, Inc., San Jose, California).

RESULTS

Hand sections and digital illustrations of representative transverse sections are presented in Figure 7 Qualitative features of the vasculature, mesophyll, bundle sheaths, epidermis, and cuticle were found. Details in higher resolution are presented in Figures 2 and 3.

Analyzing the Abaxial/Adaxial (ADAB) length ratios of transverse sections of leaves, we found that *Uniola paniculata, Ammophila breviligulata*, and *Spartina alterniflora* did not differ significantly from each other, but were significantly different from all other species. *Juncus gerardii* and *Phragmites australis* were significantly different from each other and all other species. Results of Tukey test with connecting letters report is shown in Figure 8. N-values were from 3–6.

Although the range of vascular bundle transverse section areas (AVB) was 2,000–12,000 μm^2, few significant differences were observed. Significant differences were assumed for all p-values less

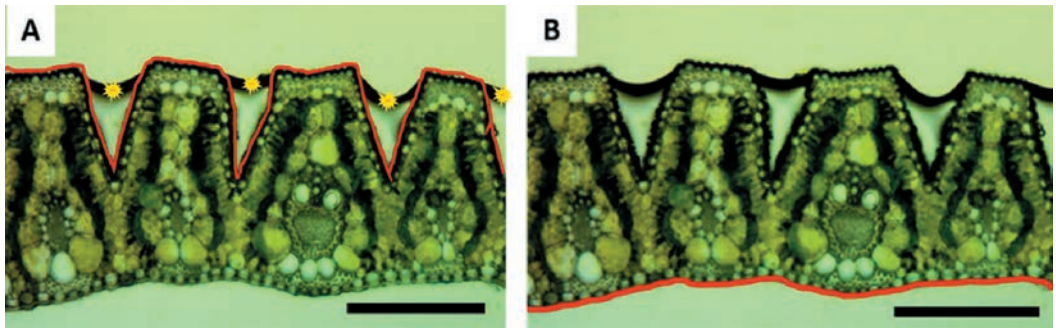

Figure 4. Leaf sections of *Spartina alterniflora* using the freehand tool in ImageJ to measure the length of adaxial (A) and abaxial (B) sides of transverse leaf sections to determine the ADAB ratio [adaxial length/abaxial length] for each species (N=3–6 for each species). Black scale bar is 200µm. Yellow stars indicate water artifact that was excluded from measurements.

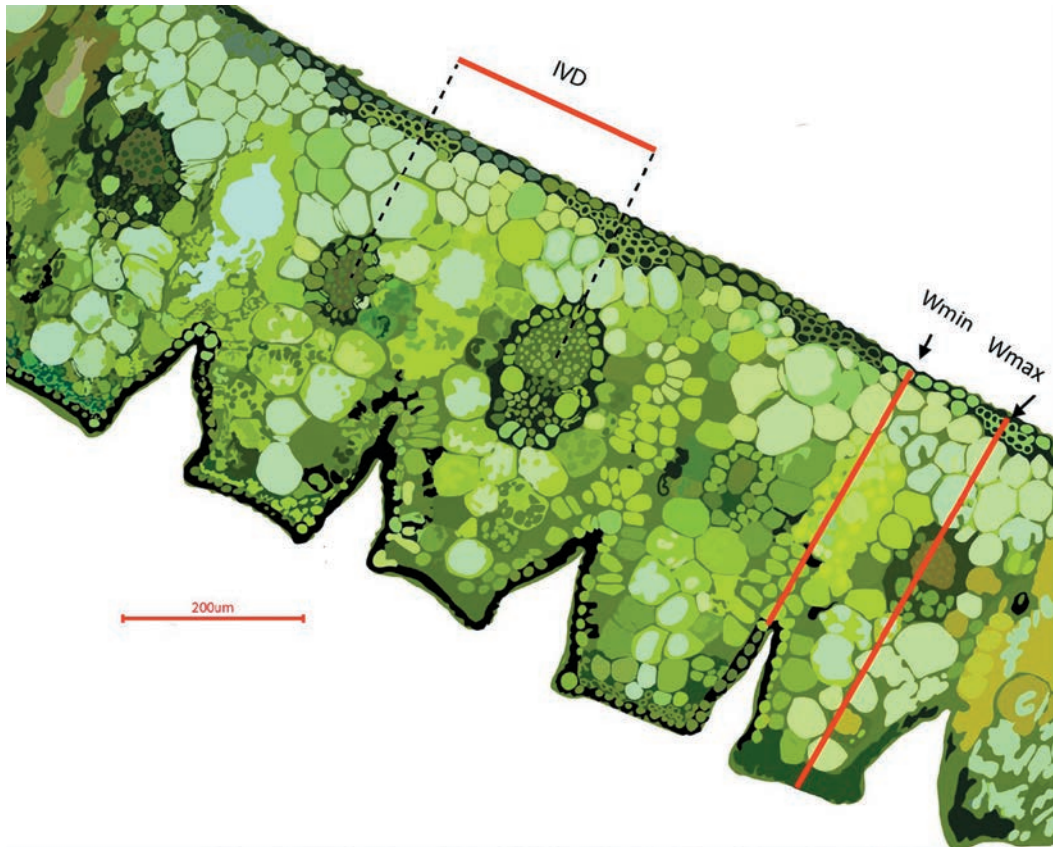

Figure 5. Adobe illustrator rendition of transverse section of *Spartina alterniflora* leaf blade with true scale (created with layering) to show how Wmax, Wmin, and IVD were measured in ImageJ. Wmax is maximum width, Wmin is minimum width, and IVD is interveinal distance. Labels are on the abaxial side of the leaf.

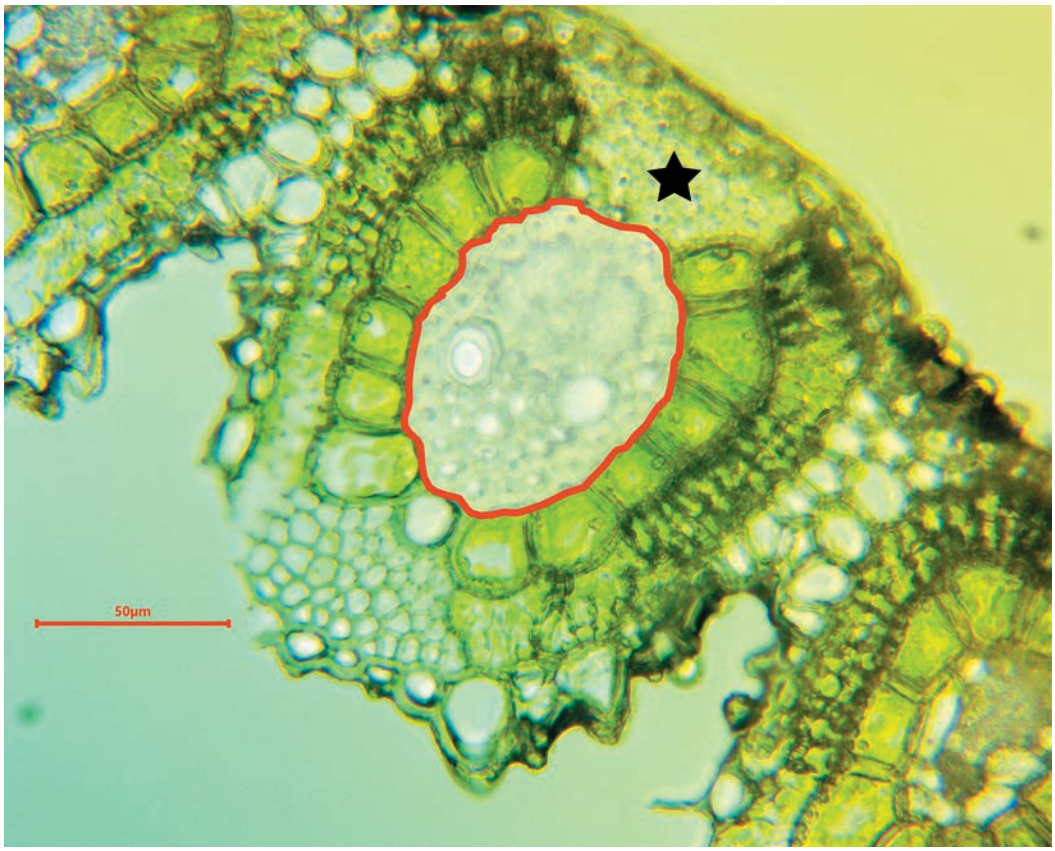

Figure 6. Leaf section of *Distichlis spicata* using the freehand tool in ImageJ to measure area of vascular bundles (AVB). Fibers around vascular tissue were included, but bundle sheath was not. The abaxial side of the leaf is indicated with a star in the sclerenchyma girdle.

than 0.05. A Tukey test found significant differences between *Juncus gerardii,* and *Phragmites australis* and *Distichlis spicata*. Large variance was observed in all samples. This is likely related to changes taking place during leaf development, growth, and patterning. Larger vascular bundles are positioned toward the midrib, and VBs increase in size toward the culm. This may be a subject of future study. N-values ranged from 10–28. A complete connecting letters report is included in Figure 9.

Average interveinal distances (IVD) ranged from about 175–300 µm. *Uniola paniculata* (UNPA) was significantly different from all other species, and details of significance of other relationships are presented in Figure 10 with a connecting letters report. N-values ranged from 10–22.

Average minimum leaf width (Wmin) and maximum leaf width (Wmax) were significantly different for all individual species. A connecting letters report from JMP is presented for Wmax and Wmin comparisons for different species in Figure 11. N-values ranged from 7–27.

DISCUSSION

Anaotomy of these plants has been carefully studied, and much more information about structure-function relationships regarding them is available (Dengler et al. 1994; Nyakas and Kalapos 1996; Maricle et al. 2009). Metcalfe (1960) includes illustrations based on microscopy for some of the genera discussed here, but he did not include any of the American species that we investigated.

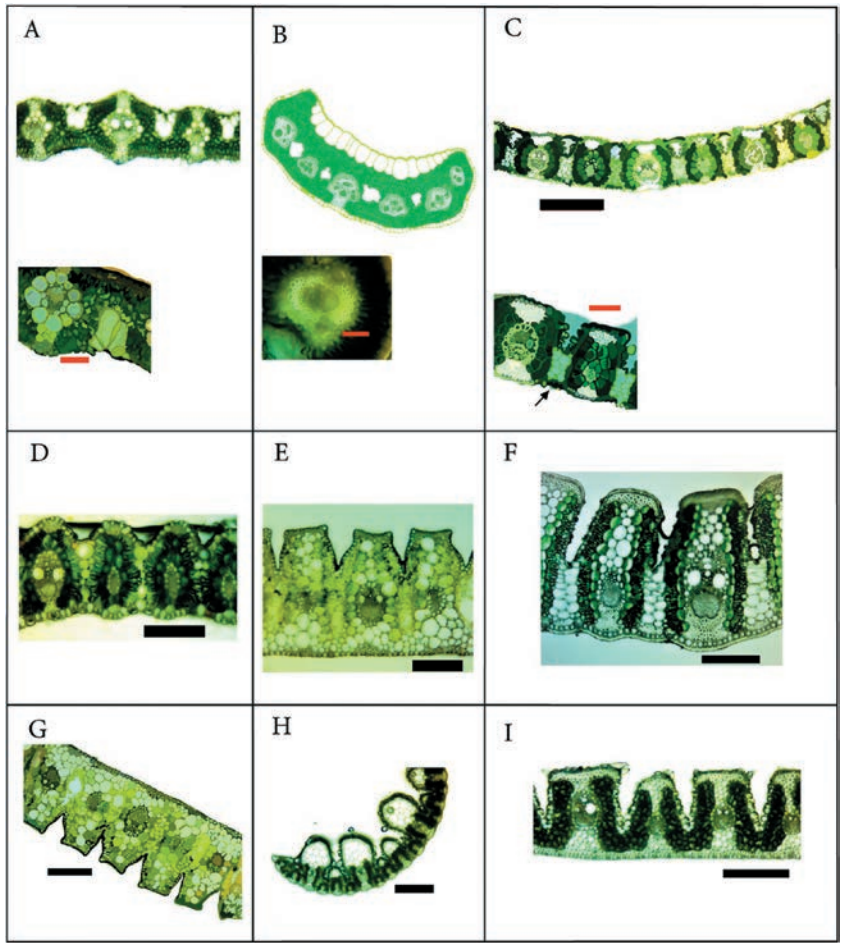

Figure 7. Examples of leaf cross sections. Some water artefacts are retained in art and imaging, as they are a common feature using this method. Black bars are 200µm, red bars are 50m. **A.** *Phragmites australis,* C3 photosynthesis. Note low ADAB ratio and paucity of chloroplasts in bundle sheaths. Insert is created in illustrator and highlights bulliform cells of adaxial epidermis, which are grouped and regularly spaced. Mesophyll cells are lobed. Insert scale bar is 50µm. **B.** *Juncus gerardii,* C3 photosynthesis. Illustrator diagram is somewhat transparent, and can be used as a tool with layering to see ratios at any size or field of view. Adaxial epidermal cells are columnar and bulliform in nature with significant cuticle. Aerenchyma air spaces are present between vascular bundles. Insert highlights unusual vasculature structures lateral to main bundles. **C.** *Distichlis spicata,* C4 photosynthesis. Both images created in Illustrator with true scale. Note Kranz anatomy, salt glands (More details in Figure 2), irregular structures in cuticle, and fibers in phloem. **D.** *Panicum amarum,* C4 photosynthesis. Vascular bundles are ovoid, and display Kranz anatomy. Each is tipped with a fiber bundle,referred to as a girdle in Metcalfe (1960), and irregularly shaped epidermal cells. Cuboidal silica bodies and oil bodies are present in bundle sheath cells. Bulliform cells are regularly shaped and arranged with one larger spherical cell flanked by two smaller ones. Chlorenchyma cells of mesophyll are radiate. Water artefact is present on adaxial side of leaf. **E.** *Spartina alterniflora*, C4 photosynthesis. Note Kranz anatomy, large ADAB index and bundle sheath extension cells populated with chloroplasts. Stomata are only present on the adaxial side of the leaf, so the mechanical rolling mechanism provided by structure reduces water loss in fluctuating habitat. **F.** *Uniola paniculata* C4. Note longitudinal extension of bundle sheath in Kranz anatomy, stacking of chloroplasts (possibly artefact) in BS cells, regular thickness of cuticle on abaxial epidermis, colorless parenchyma cells separating mesophyll cells between bundles, and large Wmax values. **G.** Artist's rendition of *S. alterniflora* (also see Figure 7). **H.** *Spartina patens*, C4 photosynthesis. Note dimorphic nature of leaf, extensive colorless parenchyma cells, alternating large and small vascular bundles, cuticular details on adaxial side of leaf, Kranz anatomy. Higher magnification detail in Figure 3. Some water artefact was removed in Adobe Illustrator. **I.** *Ammophila breviligulata*, C3 photosynethesis. Note large lumens of fibers of abaxial fiber girdle, large ADAB ratios, trichomes on adaxial side of leaf, absence of Kranz anatomy.

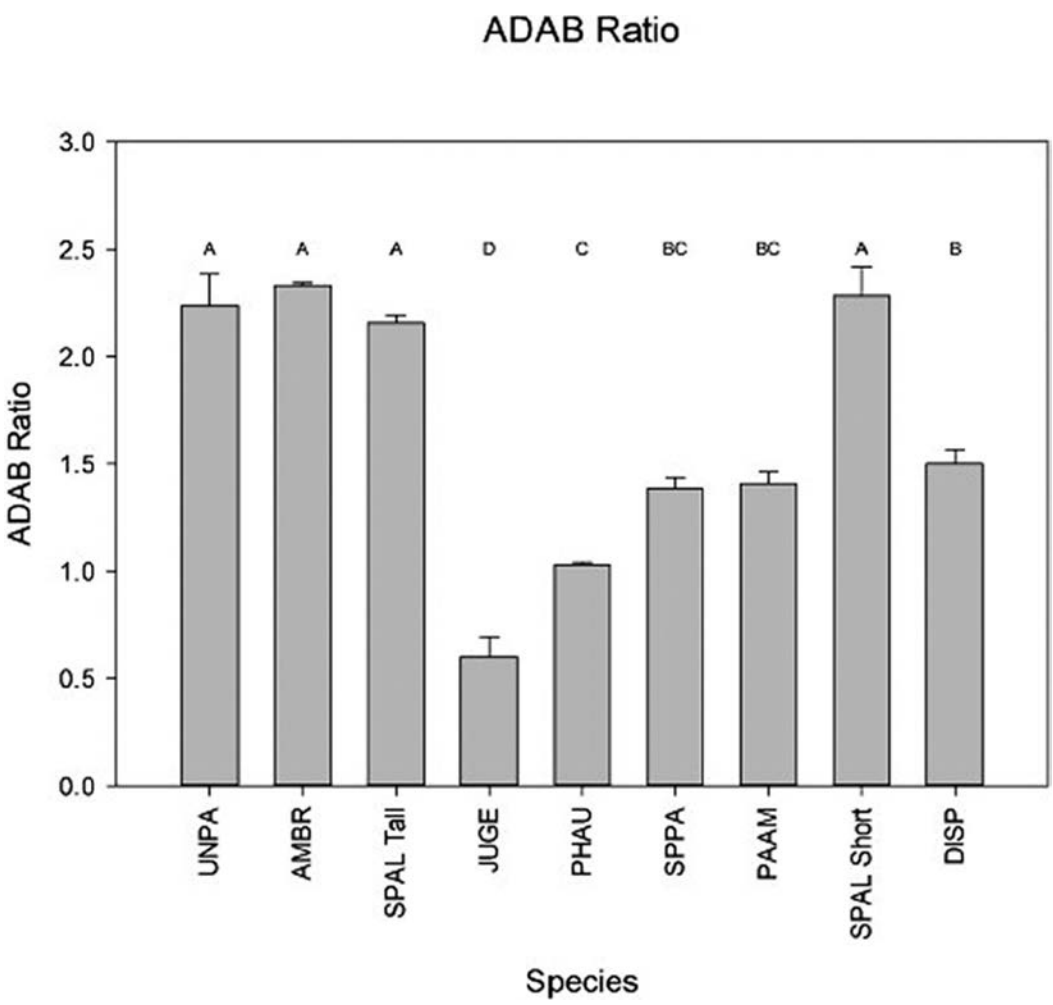

Figure 8. Average ADAB ratios ± 1 SD. Significant differences in ADAB ratios were found between the indicated species (N values ranged from 3–6). Species not connected by the same letter are significantly different.

Employing readily available methods, we present anatomical data on some of these coastal grass community members as a practical and useful resource for identification, which will be useful in plant community assessment and conservation and restoration efforts. Although hand-sectioning has limitations, many structures like silica bodies and chloroplasts can be visualized with fewer artifacts and better color retention than with embedding techniques. Moreover, our method is much more rapid and inexpensive than others and does not require any specialized equipment and, therefore, may be useful to a wider array of workers.

Our IVD measurements are not exact, as we measured from our best "by eye" estimate of the middle of the phloem of one vascular bundle to the next. Using a more time-consuming process of finding the actual geometric center did not make enough of a difference in our measurements to warrant the extra time it required and the subsequent reduction of N-values.

ADAB ratios are hypothesized to be related to the relationship between Wmin and Wmax in our data, and we found this to be the case (See Figures 10 and 11). ADAB ratios are very useful; The greater the ADAB ration, the greater the difference in the shapes of the upper and lower surfaces

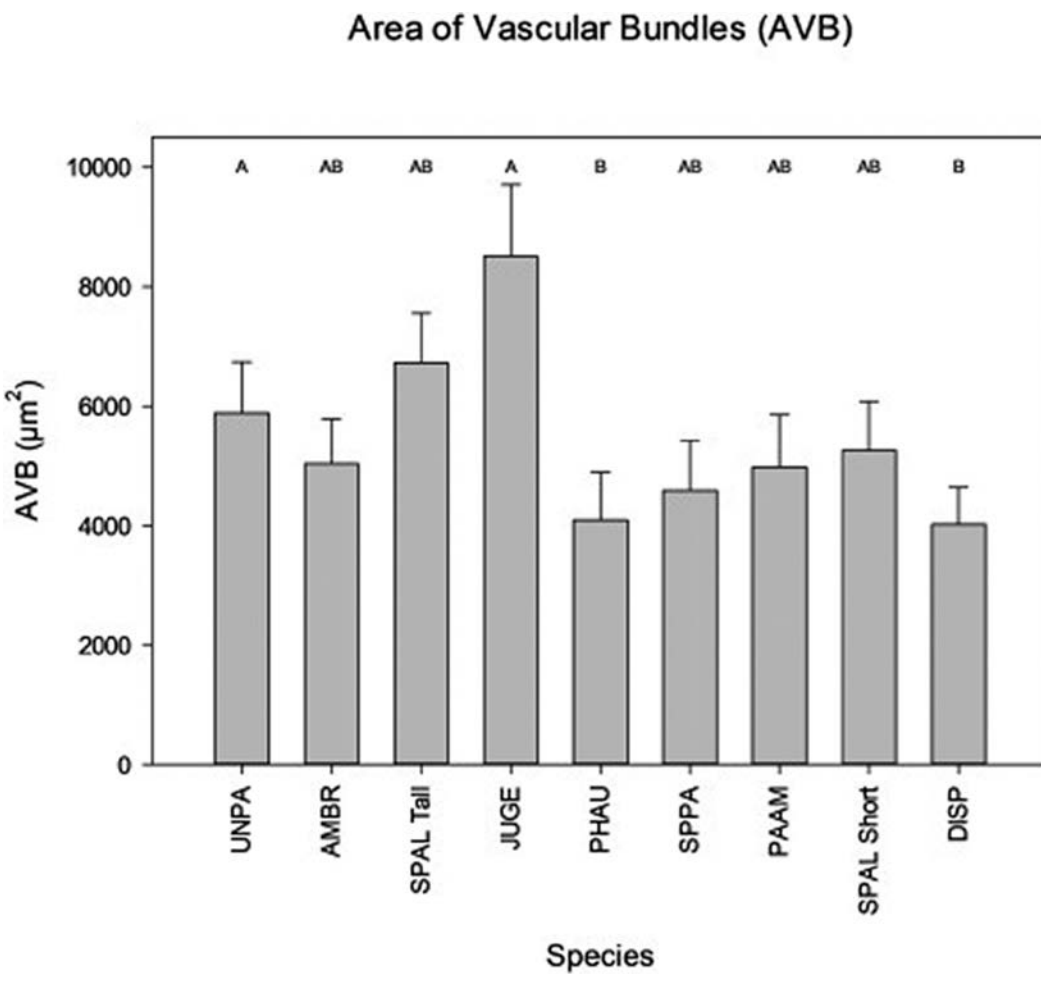

Figure 9. Range of vascular bundle transverse section areas (AVB) was 2,000–12,000 µm^2. Averages are shown with ± 1SD. Few significant differences were observed. A Tukey test revealed only that JUGE differed from PHAU (p=0.03) and DISP (p=0.03), and high variance was observed in all samples. This is likely related to leaf patterning. Larger vascular bundles are positioned toward the midrib, and VBs increase in size toward the culm. This may be a subject of future study. N-values ranged from 10–28

of the leaf. This ratio also indicates the capacity for tightness of the rolling of the leaf and, hence, its effectiveness in reducing the surface area to volume ratio during times of stress. *Spartina alterniflora*, for example, only has stomata on the adaxial side of the leaf (Maricle et al. 2009), and its markedly higher ADAB ratios are indicative of its specialized physiology.

Cross-sectional areas of vascular bundles could be affected by angle of cut, as sections are not always perfectly straight. However, our hand sections are straight enough to provide useful measurements if at least three vascular bundles are brought into focus without stacking with a 10× objective lens. The variance of this parameter was very high (Figure 9) and only a few significant differences were found. This is likely because vascular bundles near the middle of the leaf blade are larger than those near the edges, which is an intriguing area of further study of plant development and hydrodynamics.

Color was somewhat affected by the digital camera in certain images. This effect is hard to

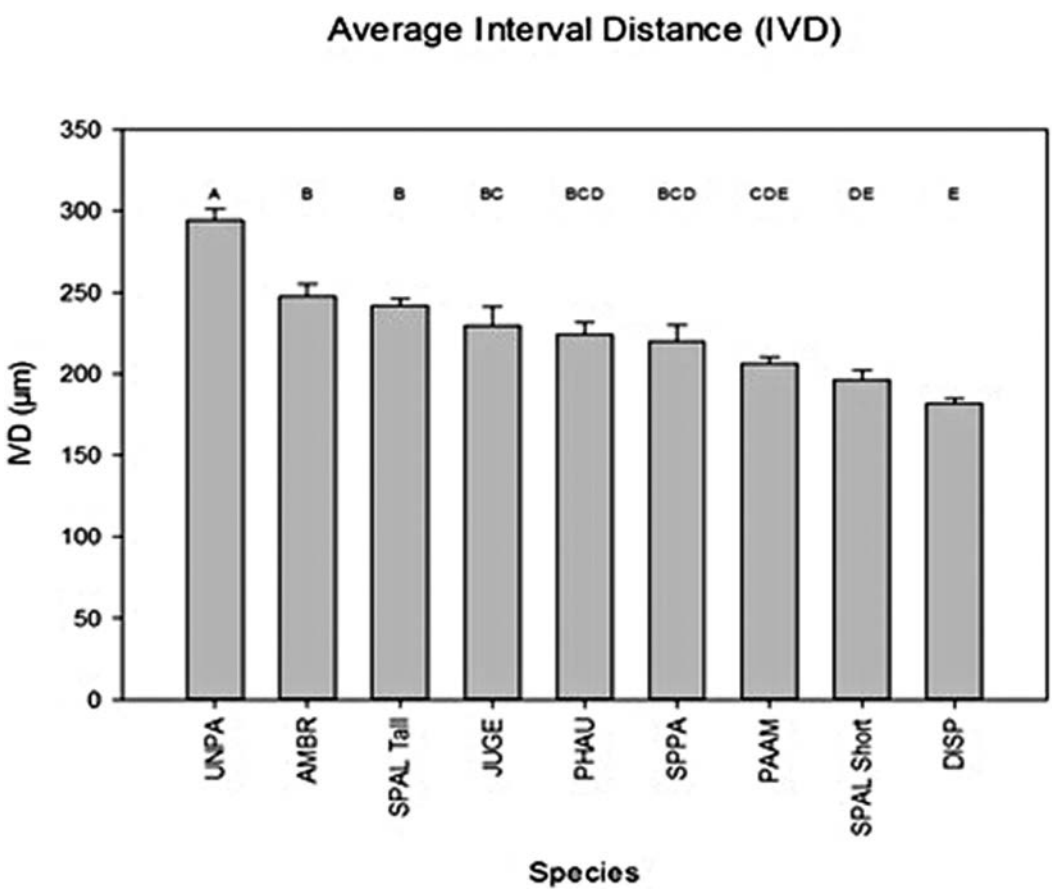

Figure 10. Average interveinal distances (IVD) with ± 1SD. Species that are not connected by a letter were significantly different from each other, as derived by Tukey post-test. *Uniola paniculata* (UNPA) was significantly different from all other species. N-values ranged from 10–22.

describe in quantitative terms, but the greens appear a bit darker with the camera than with the naked eye, or even with a cell phone camera. This was somewhat resolved by the artists' pallet work in Adobe Illustrator.

In many images, water artifacts are present. These are hard to exclude, because of the irregular shapes of the transverse sections and the minimal processing of the samples. Because they are generally present and appear very similar in many preparations, we feel that they do not detract from the images presented in this paper and may even be helpful, since other workers who use this method will see similar artifacts in their preparations.

Despite the limitations of our method, we propose that it is nonetheless of value for the practicality that it offers. Conservation and restoration efforts that involve these species may be enhanced and expedited by these tools, which is important, as the ecosystem services provided by these plants have high economic and ecological value. Sea level rise is occurring at an accelerating pace, and every effort must be made to preserve these ecosystems and the species that depend on them.

Although certain of these species have more cosmopolitan ranges than others, the anatomical species concept is most useful when considered in conjunction with the ecological and morphological species concepts, as we only compare these grasses to their associated species in north and mid-Atlantic U.S. coastal ecosystems.

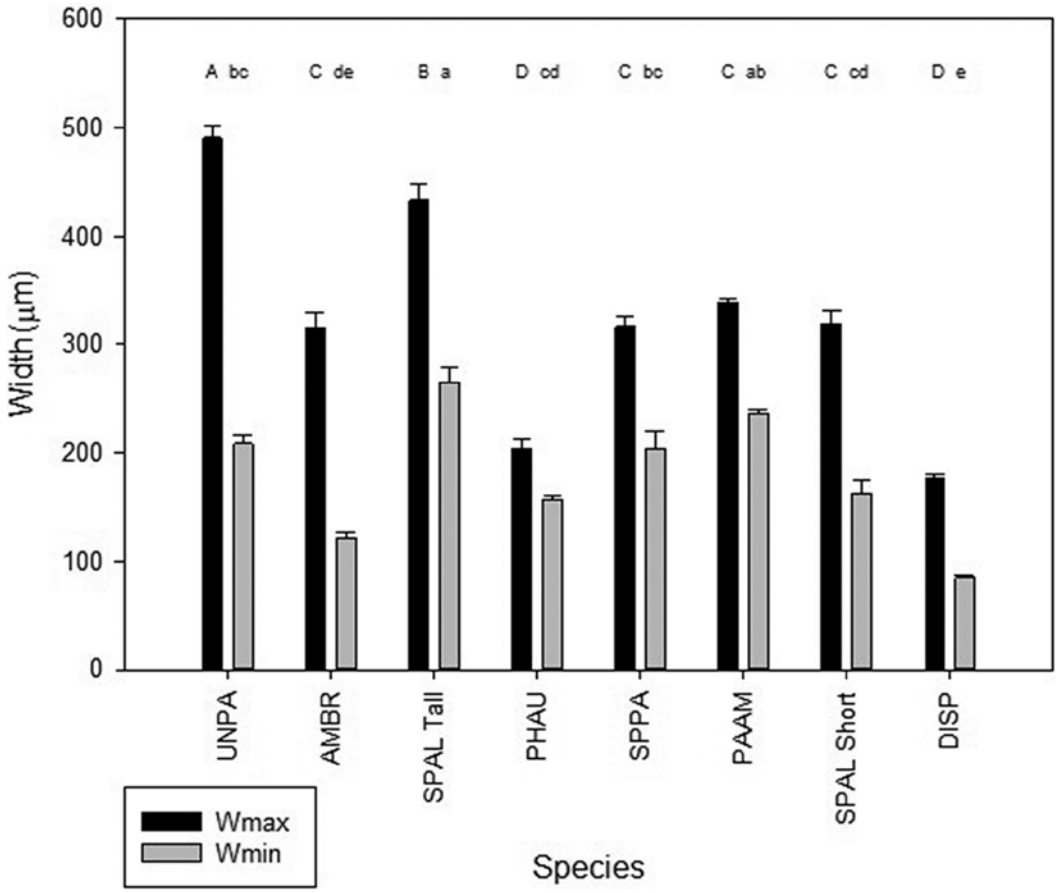

Figure 11. Average minimum leaf width (Wmin) and maximum leaf width (Wmax) with ± 1SD. Differences between Wmax and Wmin were significant for each species. Connecting letters report from JMP is noted for Wmax and Wmin comparisons for different species. N-values ranged from 7–27.

ACKNOWLEDGMENTS

We thank Gerald Edwards and Nouria Koteyeva for helpful consultations about vascular anatomy and C4 photosynthesis. We also thank Julie Zinnert for providing material of *Panicum amarum* and *Uniola paniculata* and help with identification.

LITERATURE CITED

Aracama, C.V., M.E. Kane, S.B. Wilson, and N.L. Philman. 2008. Comparative growth, morphology, and anatomy of easy- and difficult-to-acclimatize Sea Oats (*Uniola paniculata*) genotypes during in vitro culture and ex vitro acclimatization. J. Amer. Soc. Hort. Sci. 133:830–843.

Baisakh, N., M.V. RamanaRao, K. Rajasekaran, P. Subudhi, J. Janda, D. Galbraith, C. Vanier, and A. Pereira. 2012. Enhanced salt stress tolerance of rice plants expressing a vacuolar H^+-ATPase subunit c1 (SaVHAc1) gene from the halophyte grass *Spartina alterniflora* Löisel. Plant Biotechnol. J. 10:453–464.

Barbier, E.B., S.D. Hacker, C. Kennedy, E.W. Koch, A.C. Stier, and B.R. Silliman. 2011. The value of estuarine and coastal ecosystem services. Ecol. Monogr. 81:169–193.

Charbonneau, B.R. and R.A. Balsamo. 2015. Greenhouse growth of native American beachgrass (*Ammophila breviligulata*) and invasive asiatic sand sedge (*Carex kobomugi*) under competition. Res. J. Bot. 10:61–72.

Chen, Q.K., B. Chen, H. Lu, H. Zhou, and Z. Mei. 2015. An innovative strategy for reciprocal distant hybridization between *Spartina alterniflora* and rice. Agric. Sci. Technol. 16:2604–2611.

Christian, D.G., A.B. Riche, and N.E. Yates. 2002. The yield and composition of switchgrass and coastal panic grass grown as a biofuel in Southern England. Bioresource Technol. 83:115–124.

Chung C.H. 2006. Forty years of ecological engineering with *Spartina* plantations in China. Ecol. Engin. 27:49–57.

Crain, C.M., B.R. Sillman, S.L. Bertness, and M.D. Bertness. 2004. Physical and biotic drivers of plant distribution across estuarine salinity gradients. Ecology 85:2539–2549.

Dengler, N.G., R.E. Dengler, P.M. Donnelly, and P.W. Hattersley. 1994. Quantitative leaf anatomy of C3 and C4 grasses (Poaceae): bundle sheath and mesophyll surface area relationships. Ann. Bot. 73:241–255.

Eid, E.M., K.H. Shaltout, Y.M. Al-Sodany, S.A. Haroun, T.M. Galal, H. Ayed, K.M. Khedher, and K. Jensen. 2020. Seasonal potential of *Phragmites australis* in nutrient removal to eliminate the eutrophication in Lake Burullus, Egypt. J. Freshwater Ecol. 35:135–155.

Feagin. R.A., J. Figlus, J.C. Zinnert, J. Sigren, M.L. Martínez, R. Silva, W.K. Smith, D. Cox, D.R. Young, and G. Carter. 2015. Going with the flow or against the grain? The promise of vegetation for protecting beaches, dunes, and barrier islands from erosion. Frontiers Ecol. Environ. 13:203–210

Futorna, O. and I. Olshanskyi. 2013. Micromorphology of the halophyte *Juncus gerardii* Loisel. subsp. *gerardii*. Modern Phytomorphology 4:341–348.

Grigiore, M-N. and C. Toma. 2011. Ecological implications of bulliform cells on halophytes, in salt and water stress natural conditions. Studia Universitatis "Vasile Goldiș", Seria Științele Vieții 21:785–792.

Guda, M., M. Taher, and B. Almayahi. 2019. Anatomical characteristics of vascular bundles associated with heat tolerance in *Phragmites australis*. Analele Universității din Oradea, Fascicula Biologie 26:136–139.

Hacker, S.D., K.R. Jay, N. Cohn, E.B. Goldstein, P.A. Hovenga, M. Itzkin, L.J. Moore, R.S. Mostow, E.V. Mullins, and P. Ruggiero. 2019. Species-specific functional morphology of four U.S. Atlantic coast dune grasses: biogeographic implications for dune shape and coastal protection. Diversity 11:82.

Hansen, D.J., P. Dayanandan, P.B. Kaufman, and J.D. Brotherson. 1976. Ecological adaptations of salt marsh grass, *Distichilis spicata* (Gramineae), and environmental factors affecting its growth and distribution. Amer. J. Bot. 63:635–650.

Litalien, A.A.S., A. Rutter, and B.A. Zeeb. 2020. The impact of soil chloride concentration and salt type on the excretions of four recretohalophytes with different excretion mechanisms. Int. J. Phytoremed. 22: 1122–1128.

Lonard, R.I. and F.W. Judd. 2011. The Biological Flora of Coastal Dunes and Wetlands: *Panicum amarum* S. Elliott and *Panicum amarum* S. Elliott var. *amarulum* (A.S. Hitchcock and M.A. Chase) P. Palmer. J. Coastal Res. 27:233–242.

Maricle, B.R., N.K. Koteyeva, E.V. Voznesenskaya, J.R. Thomasson, and G.E. Edwards. 2009. Diversity in leaf anatomy, and stomatal distribution and conductance, between salt marsh and freshwater species in the C4 genus *Spartina* (Poaceae). New Phytol. 184:216–233.

Mehaffey, M.H., D.S. Fisher, and J.C. Burns. 2005. Photosynthesis and nutritive value in leaves of three warm-season grasses before and after defoliation. Agronomy J. 97:755–759.

Metcalfe, C.R. 1960. Anatomy of the monocotyledons. Volume 1: Gramineae. Oxford University Press, Clarendon, Oxford, U.K.

Morris, L., K. Yun, A. Rutter, and B.A. Zeeb. 2019. Characterization of excreted salt from the recretohalophytes *Distichilis spicata* and *Spartina pectinata*. J. Environ. Qual. 48:1775–1780.

Nyakas, A. and T. Kalapos. 1996. Variation in C4 type leaf anatomy in the Hungarian angiosperm flora. Abstracta Botanica 20:93–104.

Ohsugi, R. and T. Murata. 1986. Variations in the leaf anatomy among some C4 *Panicum* species. Ann. Bot. 58:443–453.

Rozema, E.R., R.J. Gordon, and Y. Zheng. 2014. Plant species for the removal of Na^+ and Cl^- from greenhouse nutrient solution. HortScience 49:1071–1075.

Saltonstall, K. 2002. Cryptic invasion by a non-native genotype of the common reed, *Phragmites australis*, into North America. Proc. Natl. Acad. Sci. (USA) 99:2445–2449.

Savage, J.A., S.D. Beecher, L. Clerx, J.T. Gersony, J. Knoblauch, J.M. Losada, K.H. Jensen, M. Knoblauch, and N.M. Holbrook. 2017. Maintenance of carbohydrate transport in tall trees. Nature Plants 3:965–972.

Semenova, G.A., I.R. Fomina, and K.Y. Biel. 2010. Structural features of the salt glands of the leaf of *Distichlis spicata* 'Yensen 4a' (Poaceae). Protoplasma 240:75–82.

Soukup, A. and E. Tylová. 2014. Essential methods of plant sample preparation for light microscopy. Methods Mol. Biol., 1080. (doi: 10.1007/978-1-62703-643-6_1).

Srinivas, A., G. Rajasheker G. Jawahar, P.L. Devineni, M. Parveda, S.A. Kumar, P.B. Kavi Kishor. 2018. Deploying mechanisms adapted by halophytes to improve salinity tolerance in crop plants: Focus on anatomical features, stomatal attributes, and water use efficiency. pp 41–64 *In*: Kumar, V., S. Wani, P. Suprasanna, and L.S. Tran (eds.). Salinity Responses and Tolerance in Plants, Volume 1. Springer, Cham, Switzerland.

Tiner, R.W. 1987. A field guide to the coastal wetland plants of the northeastern United States. University of Massachusetts Press. Amherst, Massachusetts.

Toyama, T., T. Furukawa, N. Maeda, D. Inoue, K. Sei, K. Mori, S. Kikuchi, and M. Ike. 2011. Accelerated biodegradation of pyrene and benzo[a]pyrene in the *Phragmites australis* rhizosphere by bacteria-root exudate interactions. Water Research 45:1629–1638.

Watson, E.B., C. Wigand, M. Censer, and K. Blount. 2014. Inundation and precipitation effects on growth and flowering of the high marsh species *Juncus gerardii*. Aquatic Bot. 121:52–56.

Ye, W., T. Wang, W. Wei, S. Lou, F. Lan, S. Zhu, Q. Li, G. Ji, C. Lin, X. Wu, and L. Ma. 2020. The full-length transcriptome of *Spartina alterniflora* reveals the complexity of high salt tolerance in monocotyledonous halophyte. Plant Cell Physiol. 61:882–896.